Gwon *et al. Int J Concr Struct Mater* (2023) 17:5
https://doi.org/10.1186/s40069-022-00565-1

International Journal of Concrete Structures and Materials

RESEARCH Open Access

Rheological and Mechanical Properties of Kenaf and Jute Fiber-Reinforced Cement Composites

Seongwoo Gwon[1,4†], Seong Ho Han[2†], Thanh Duc Vu[3], Chanyoung Kim[3] and Myoungsu Shin[3*]

Abstract

This study investigated the rheological and mechanical properties of cement composites with kenaf and jute fibers for use in shotcrete. The length and volume fractions of the fiber were varied; the rheological properties were analyzed in terms of air content, compression and flexural tests were conducted, and the degree of fiber dispersion was assessed using fluorescence microscopy. The rougher surfaces of the jute fibers led to a higher yield stress and viscosity of the composite compared to the kenaf fibers. The use of 10-mm-long jute fibers at 2.0% volume fraction led to optimal rheological properties while 30-mm-long jute fibers at 1.0% resulted in the worst properties. The yield stress and plastic viscosity exhibited positive and negative correlations with the fiber volume fraction, respectively. This was likely because of the bridging and fluid actions of the bubbles at higher fiber content. For a given fiber content, only the yield stress increases with an increase in fiber length. Although all the mechanical properties deteriorated (compressive strength decreased from 27.5 to 6 MPa, and flexural strength deteriorated from 6.2 to 1.8 MPa), the mixtures failed in a ductile manner. Using 10-mm-long kenaf fibers at 2.0% induced optimal fiber dispersion, whereas the minimum dispersion-coefficient value was found for 5-mm-long kenaf fibers at 0.5%.

Keywords: Fresh concrete, Kenaf, Jute, Rheological properties, Compressive strength

1 Introduction

Recently, the demand for sustainable construction materials is increasing, particularly with the aim of reducing CO_2 emissions. One of the emerging approaches to this problem is to incorporate plant-based fibers, such as kenaf, hemp, and jute, into polymer composites or concrete. This can enhance the strain capacity, toughness, and crack resistance under tension (Elsaid et al., 2011; Ramakrishna & Sundararajan, 2005). Natural fibers are affordable and promising renewable resources that can enhance the mechanical properties of concrete (Chin & Yousif, 2009; Roma et al., 2008). Many studies on natural fiber-reinforced cement composites (NFRCCs) have been performed, and these have examined the mechanical properties (Fan et al., 2012; MacVicar et al., 1999), cement hydration (Gwon et al., 2021; Vaickelionis & Vaickelioniene, 2006), setting time (Choi & Choi, 2021; Gwon et al., 2021), and internal curing (Dávila-Pompermayer et al., 2020; Jongvisuttisun et al., 2018) of composite materials, as well as the use of different surface treatments for natural fibers (Li et al., 2007; Valadez-Gonzalez et al., 1999). Specifically, kenaf and jute fibers, which are classified as bast fibers, are the most popular natural materials in this field because of their abundancy in Asia-Pacific countries and the United States (Market Research Future, 2020) and these fibers have relatively high tensile strength compared to other types of natural fibers (Li et al., 2007; Saheb & Jog, 1999). Many studies

†Seongwoo Gwon and Seong Ho Han have contributed equally to the work

Journal information: ISSN 1976-0485 / eISSN 2234-1315

*Correspondence: msshin@unist.ac.kr

[3] Department of Urban and Environmental Engineering, Ulsan National Institute of Science and Technology (UNIST), 50 UNIST-Gil, Ulsan 44919, Republic of Korea
Full list of author information is available at the end of the article

have also been conducted on NFRCCs that incorporate hemp (Awwad et al., 2012; Li et al., 2004), sisal (de Andrade Silva et al., 2010; Wei & Meyer, 2014), coir (Li et al., 2006), banana (Zhu et al., 1994), and flax (Sawsen et al., 2014, 2015) fibers.

Due to their hygroscopic characteristics, the water absorption capacity of natural fibers is crucial for the production of concrete (Gwon et al., 2021; Jongvisuttisun et al., 2018). If the exact amount of water absorbed by natural fibers is considered as additional water in the mix proportions, the reduction in concrete workability owing to the loss of mix water by the fibers can be avoided (Jongvisuttisun et al., 2018). However, few studies have quantitatively explored this issue (Gwon & Shin, 2021; Gwon et al., 2021). Gwon et al., (2021) estimated the water absorption capacity of kenaf microfibers using vacuum membrane filtration method. They found that mortar mixtures containing kenaf microfibers in the saturated surface dry (SSD) condition had a similar range of flow diameters, albeit with different fiber contents. Thus, the mix water quantity remained unchanged in the fresh mortar mixture, aside from the portion of the microfibers. Furthermore, Gwon and Shin, (2021) determined that the rheological properties of cement pastes could be modified using kenaf microfibers under SSD conditions. However, aside from that of Yun et al., (2022), there have been no rheological studies examining natural fiber-reinforced concrete, including coarse aggregates.

One of the possible applications of NFRCCs is shotcrete. Several researchers have used hemp fibers in concrete and shotcrete (Morgan et al., 2017), and the resulting materials exhibited reduced plastic and drying shrinkage compared to those using steel or polypropylene fibers. Shotcrete is a mortar or concrete pneumatically projected onto a surface using a hose at a construction site (Banthia, 2019). Thus, shotcrete typically needs to have relatively low plastic viscosity and high yield stress. It is assumed that such requirements can be met by incorporating natural fibers in cement composites. When natural fibers are used in shotcrete, the water absorbed by the fibers is assumed to be squeezed out under pumping pressure. In turn, the water released from the fibers induce better pumpability. Once the mixture is cast and freed from pressure, the fibers absorb the released water again, leading to better shootability and less rebound. The absorbed water may eventually be used for internal curing (Ahn & Shin, 2018; Dávila-Pompermayer et al., 2020; Jongvisuttisun et al., 2018; Mezencevova et al., 2012). The effects of internal curing are typically evidenced by reduced autogenous shrinkage and self-desiccation in cement composites, as reported by Gwon et al., (2022). Therefore, the use of natural fibers has been observed to be advantageous for both the fresh and hardened properties of shotcrete. Among these properties, this study primarily explored the fresh properties of NFRCCs without pumping pressure by applying the rheological theory. This was a preliminary case study prior to the application of NFRCCs as shotcrete in the field.

In this study, the mechanical and rheological properties of NFRCCs were investigated using kenaf and jute fibers of varying lengths and volume fractions. In general, the use of conventional fibers (e.g., steel, glass, carbon, and polypropylene) of longer lengths and at higher volume fractions in cement composites improves their compressive and flexural behaviors (Li & Obla, 1994; Singh et al., 2019). However, the use of natural fibers of longer lengths at higher content generally causes a reduction in mechanical strength owing to the intrinsic porosity and lumen cavities (Gwon et al., 2021). Despite these drawbacks, natural fibers have beneficial effects on the rheology and hydration of cement composites and are advantageous for shotcreting because of their hygroscopic characteristics. Considering all these, the mix proportions of the NFRCCs were designed with reference to those of shotcrete. Most previous studies on NFRCCs have employed 5- to 30-mm-long chopped fibers at 0.5–3.0% by volume (Onuaguluchi & Banthia, 2016; Pacheco-Torgal & Jalali, 2011; Yun et al., 2022). Accordingly, this study limited the length and volume fraction of natural fibers to 5–30 mm and 0.5–2.0%, respectively. Rheometry and air-content tests were performed to evaluate the fresh properties of the NFRCCs, and the results of these tests were correlated. Compression and flexural tests were also performed to analyze the compressive strength, elastic modulus, and flexural strength of NFRCCs. Finally, the degree of fiber dispersion was evaluated by fluorescence microscopy.

2 Materials and Methods

2.1 Materials

Type I Portland cement, compliant with ASTM C150 (ASTM, 2020a), was used in this study. The specific gravity and specific surface area of this cement were 3.15 g/cm^3 and 2800 cm^2/g, respectively. Kenaf and jute fibers, manufactured by Soo Industry Co., Ulsan, South Korea, were used. No chemical treatment of the fibers was performed. As shown in Fig. 1, fibers were produced following a manufacturing process that consists of harvesting, water retting, decortication, and roller milling. The resulting long fibers were chopped into shorter fibers of varying lengths (5, 10, 20, and 30 mm). The densities of the completely dry kenaf and jute fibers, determined by a helium pycnometer (Amiri et al., 2017), were 1.36 g/cm^3 and 1.44 g/cm^3, respectively. Figure 2 displays all fibers with different types and lengths. Crushed coarse aggregates with a maximum size of 10 mm and a density

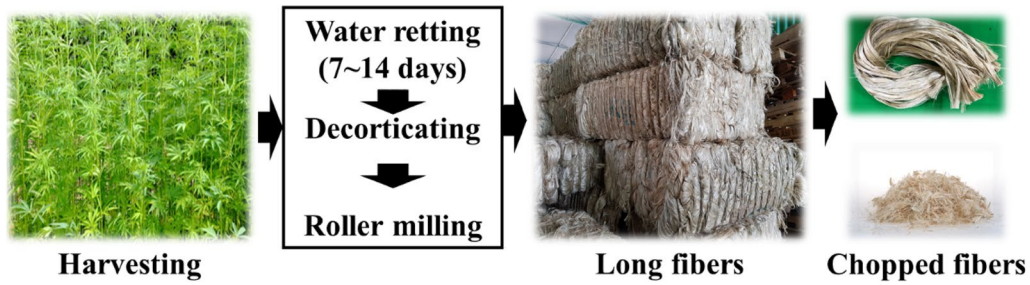

Fig. 1 Manufacturing process of plant-based natural fibers

Fig. 2 Plant-based natural fibers: **a** 5 mm kenaf; **b** 10 mm kenaf; **c** 20 mm kenaf; **d** 30 mm kenaf; **e** 5 mm jute; **f** 10 mm jute; **g** 20 mm jute; **h** 30 mm jute

of 2.51 g/cm^3 were used. Additionally, river sand (fine aggregate) with a density of 2.47 g/cm^3 and maximum size of 5 mm was used. The grading of the coarse and fine aggregates conformed to ACI 506R-16 (ACI, 2016). A polycarboxylate-based superplasticizer (specific gravity: 1.04 ± 0.05, pH: 5.0 ± 2.0) was employed.

2.2 Mix Proportions

The mix proportions of NFRCCs were designed based on the shotcrete mix cases presented by Beaupré, (1994). The main test variables were the plant type, length, and volume fraction of natural fibers. Twelve mixtures were prepared for each plant type (kenaf and jute), with fiber volume fractions ranging from 0.5 to 2.0% (Table 1). The use of 2.0% volumetric fibers was not possible for the 20- and 30-mm-long fibers, because they tended to agglomerate. Therefore, these results were excluded from the analysis.

In the mix proportions, the weight ratios of water to cement (w/c) and sand to aggregate (s/a) were fixed at 0.50 and 0.65, respectively. The percentage of superplasticizer (SP) was 2% of the cement weight. Additional water, equal to the dry weight of the fibers, was included in the effective water (w*) of the mix proportions (Table 1), and the estimation method is introduced in a later section. In other words, w*/c indicates the effective water-to-cement ratio, which considers the additional water absorbed in the prewetted fibers.

2.3 Pre-saturation Natural Fibers

Elsaid et al., (2011) reported that the incorporation of dry kenaf fibers in concrete mixtures degrades the workability of concrete owing to the partial absorption of mixing

Table 1 Mix proportions of the tested natural fiber-reinforced cement composites

Plant type	Fiber		w/c	w*/c	s/a	Unit: kg/m^3				
	Length (mm)	Vol.% (%)				w	c	FA	CA	SP
Kenaf or jute	5	0.5	0.50	0.51	0.65	246	493	961	518	9.86
		1.0		0.53						
		2.0		0.56						
	10	0.5		0.51						
		1.0		0.53						
		2.0		0.56						
	20	0.5		0.51						
		1.0		0.53						
		2.0		0.56						
	30	0.5		0.51						
		1.0		0.53						
		2.0		0.56						

w water, *w** effective water, *c* cement, *s/a* sand-to-aggregate, *FA* fine aggregate (river sand), *CA* coarse aggregate, *SP*: superplasticizer

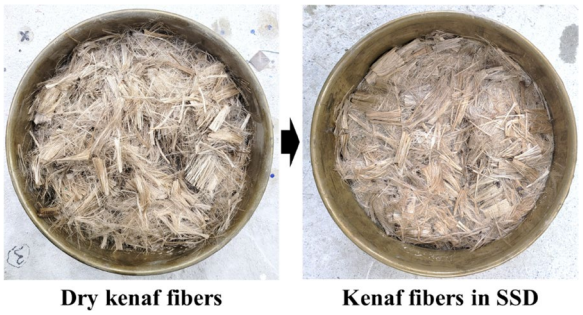

Fig. 3 Kenaf fiber sample before and after being prepared in SSD condition

water by the dry fibers. Therefore, it is critical to estimate the exact water absorption capacity of the used fibers. The water absorption capacities of the two types of fibers were estimated using the method reported by MacVicar et al., (1999). For each fiber type, at least ten samples were prepared to measure the amount of absorbed water. The original samples were dried in an oven at 80 °C for 24 h. The resulting samples were immersed in water for 24 h and immediately prepared under SSD conditions (Fig. 3). The amount of water absorbed was determined from the weight difference between the completely dry and SSD samples. It was confirmed that the two types of natural fiber absorbed the same amount of water as their dry weights; thus, the water absorption capacity of the fibers were equal to 100%.

2.4 Sample Preparation

First, both the coarse and fine aggregates were dry-mixed with the cement in a concrete mixer at a speed of approximately 50 rpm for 60 s. The mixing water and superplasticizer blend was poured into the mixing bowl and stirred for 60 s at the same speed. Subsequently, prewetted SSD natural fibers were added, and the mixture was wet-mixed at a speed of approximately 50 rpm for 30 min. The same mixing protocol was applied to all the mixtures, regardless of the length and volume fraction of the fibers. After casting the resulting mixture, as shown in Fig. 4, all samples were cured in a controlled water chamber at 20 ± 2 °C for the specified curing time.

2.5 Rheometer Tests

2.5.1 Test Procedure

An International Center for Aggregates Research (ICAR) rheometer (Koehler & Fowler, 2004), which is one of the most popular commercial models, was used in this study (Fig. 5). The radii of the cylinder and four-bladed vane were approximately 143 mm and 63.5 mm, respectively. Thus, the lateral gap between the cylinder wall and installed vane was approximately six times the maximum size of the coarse aggregate. The heights of the cylinder and vane were 305 mm and 127 mm, respectively.

As shown in Fig. 6, the rheological shearing protocol consisted of an initial breakdown step at 0.5 revolutions per second (rps) for 20 s and subsequent deceleration steps from 0.50 to 0.05 rps with each step lasting for 5 s. Only the measured shear stress–strain rate data from the deceleration steps were used for flow curve analysis. The loaded torque and vane rotation speed were simultaneously measured during the tests. Each mixture in Table 1 was tested three times. Thus, three flow curves from each

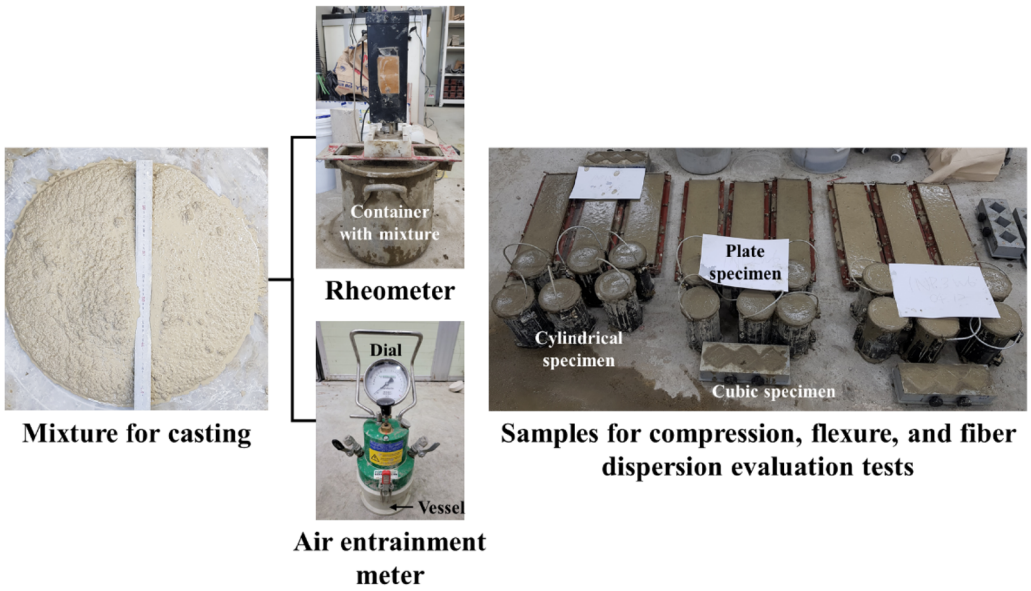

Fig. 4 Resulting mixture and samples for testing

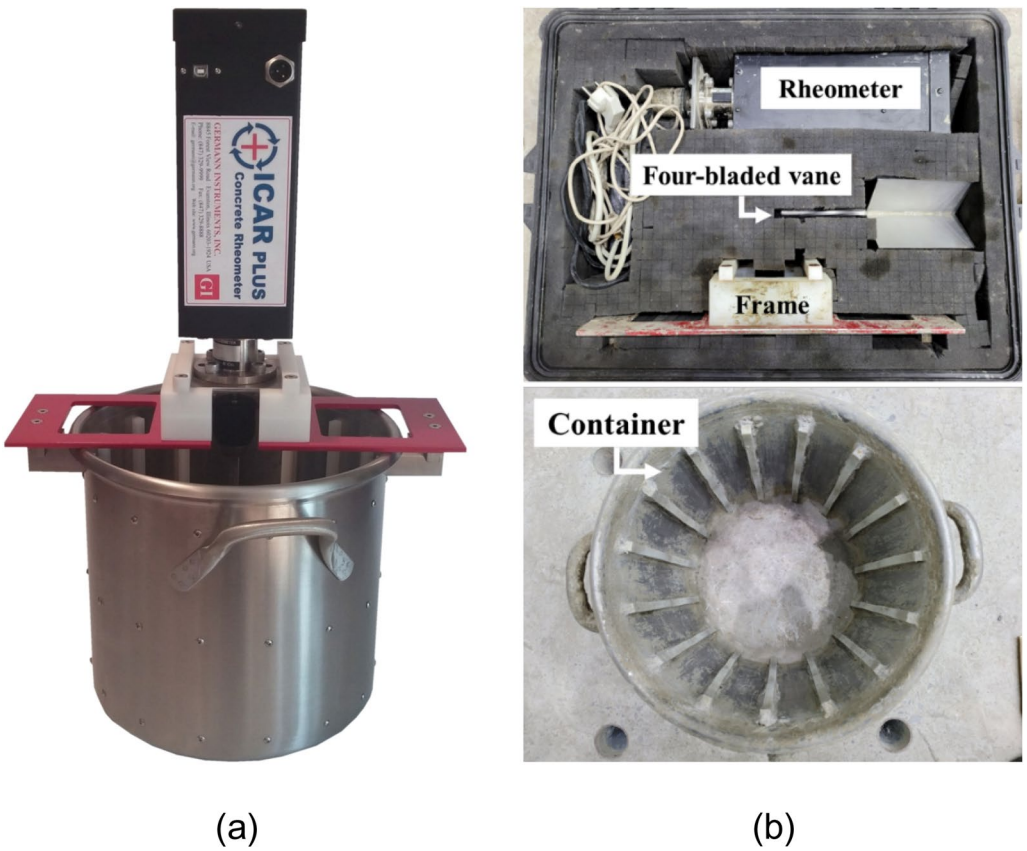

Fig. 5 ICAR rheometer (Ramakrishna & Sundararajan, 2005): **a** entire system; **b** detailed parts

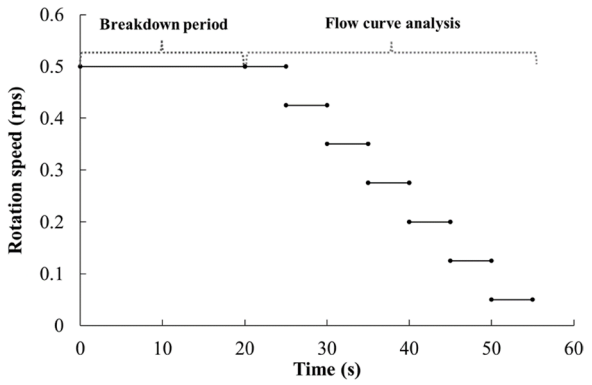

Fig. 6 Rheological shearing protocol

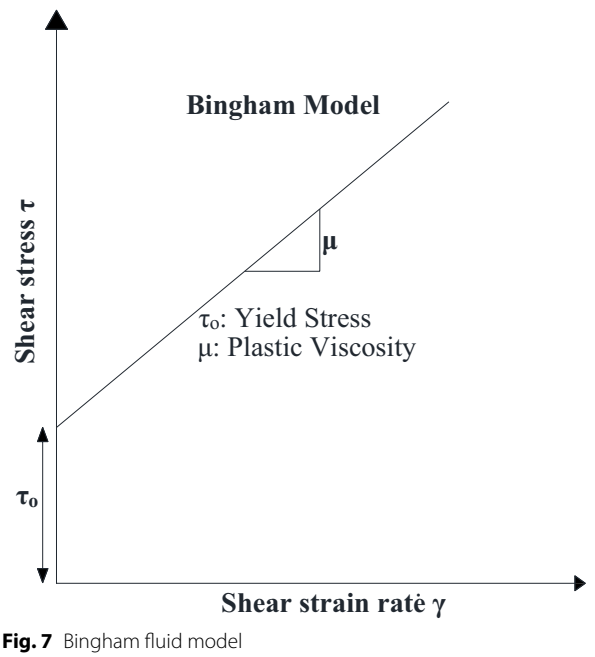

Fig. 7 Bingham fluid model

mixture were averaged to analyze the rheological properties (yield stress and plastic viscosity).

2.5.2 Flow Curve Analysis

Fresh concrete is typically assumed to behave as a Bingham fluid (Fig. 7), which means that it starts to flow once a certain level of shear stress is exerted. Accordingly, following the Bingham model, the flow behavior of fresh concrete is described by two parameters (yield stress and plastic viscosity) in Eq. (1) (Bingham, 1916): the yield stress (τ_0) signifies the minimum shear stress required for the fresh mixture to initiate its flow, and the plastic viscosity (μ) is defined as the slope of the shear stress (τ) versus the shear strain rate ($\dot{\gamma}$) curve beyond the yield stress, which is associated with the resistance to flow as

$$\tau = \mu\dot{\gamma} + \tau_0. \tag{1}$$

The Bingham model parameters were calculated based on the Reiner–Riwlin equation, which is expressed as

$$\Omega = \frac{T}{4\pi h\mu}\left(\frac{1}{{R_1}^2} - \frac{1}{{R_2}^2}\right) - \frac{\tau_0}{\mu}\ln\left(\frac{R_2}{R_1}\right), \tag{2}$$

where Ω is the rotational speed of the vane (rad/s); T is the torque applied by the vane (N·m); h is the height of the vane (m); R_1 is the vane radius (m); and R_2 is the outer container radius (m).

2.6 Air-Content Tests

The air content of the NFRCCs was measured according to ASTM C185 (ASTM, 2020b) immediately before the rheometer tests. For the air-content tests, a 400-ml vessel with a diameter of 76 mm and depth of 88 mm was filled with a mixture cast in three equal layers. Each layer was tamped 20 times around the inner surface of the vessel. The main body of the air meter was clamped tightly to the vessel (Fig. 4). The air content was read from a dial with a range of 0–50%. Kostrzanowska-Siedlarz and Gołaszewski examined the effect of the air content on the rheological properties of fresh concrete (Kostrzanowska-Siedlarz & Gołaszewski, 2015).

2.7 Mechanical Tests

After 28 days of curing, compression and flexure tests were performed only for samples containing kenaf fibers. Figure 8 shows the test setup for the compression and flexural tests. For the compression tests, at least three cylindrical samples with a diameter of 100 mm and height of 200 mm were tested for each mixture, as listed in Table 1, according to ASTM C39 (ASTM, 2020c), to analyze the compressive strength and elastic modulus. Flexure tests were conducted according to ASTM C1609 (ASTM, 2019) to assess flexural strength. Plate samples with a 25.4×128 mm^2 cross-section and 535 mm length were subjected to third-point loading. A minimum of three samples were tested for each mixture.

2.8 Fiber Dispersion Evaluation Tests

2.8.1 Test Procedure

The dispersion of natural fibers in the NFRCCs was analyzed using a fluorescence microscope (Axio Zoom.V16, Zeiss, Germany), as shown in Fig. 9. Samples in the form of 50-mm cubes were fabricated and cured for 7 days. Each sample was cut in half using a diamond saw. The

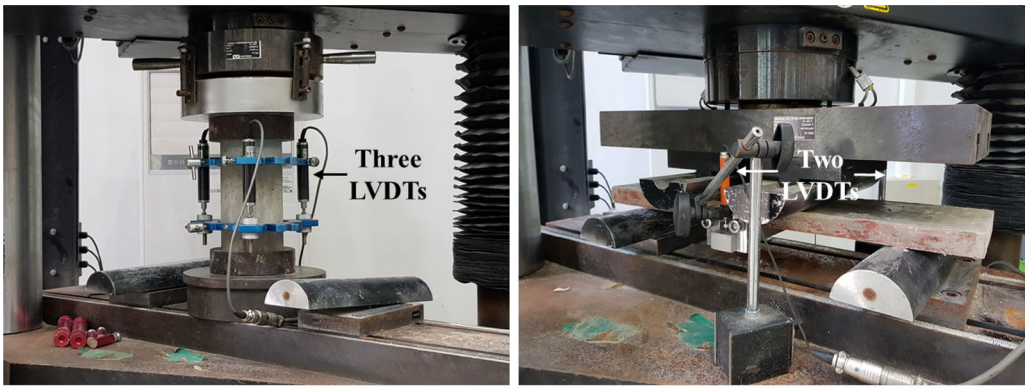

Fig. 8 Test setup for compression and flexure tests

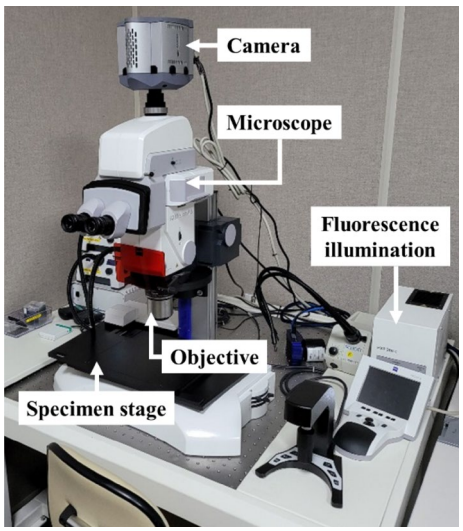

Fig. 9 Fluorescence microscope (Axio Zoom.V16, Zeiss, Germany)

cutting planes were then roughly ground and polished using sandpaper prior to the microscopic characterization. A minimum of three samples were prepared for each mixture. Thus, a total of six cross-sections were studied using the microscope for each mixture.

2.8.2 Fiber Dispersion Analysis

According to Torigoe et al., (2003), the coefficient of variation is calculated by considering the number of fibers within a certain plane, as expressed by

$$\Phi(X) = \frac{\sqrt{\frac{\sum(X_i - \overline{X})^2}{n}}}{\overline{X}}, \tag{3}$$

where n is the number of sections in a plane; $\overline{X}$ is the total number of fibers in the plane; and X_i represents the number of fibers in the i^{th} square section. In this study, each plane (50 mm × 50 mm) was divided into at least 15 sections for the analysis. The distribution coefficient, which quantitatively evaluates the degree of fiber dispersion, was calculated as follows:

$$\alpha_f = \exp[-\Phi(X)]. \tag{4}$$

The closer the distribution coefficient is to one, the better the dispersion of the fibers.

3 Results and Discussion

3.1 Rheological Properties

3.1.1 Yield Stress

For a given fiber length, the yield stress of the mixtures generally increased at higher fiber volume fractions (Fig. 10). Increasing the fiber length also led to an increase in the yield stress at a constant fiber volume fraction, regardless of the fiber type. These phenomena can be attributed to the increased interfacial friction between the matrix and fibers (Kanda & Li, 1998). Thus, the yield stresses were significantly influenced by the fiber length than the number of fibers. Similarly, Gwon and Shin, (2021) observed that the use of longer cellulose microfibers in cement paste caused larger yield stresses than the use of shorter ones. The increase in the yield stress with higher volume fraction of fiber was more marked when longer microfibers were used.

For kenaf fibers, the yield stresses ranged from 30 to 570 Pa (Fig. 10), whereas for jute fibers, the values ranged from 40 to 1400 Pa (Fig. 10). For the same length and volume fraction of fibers, the use of jute fibers led to higher yield stresses than that of kenaf fibers. This indicates that

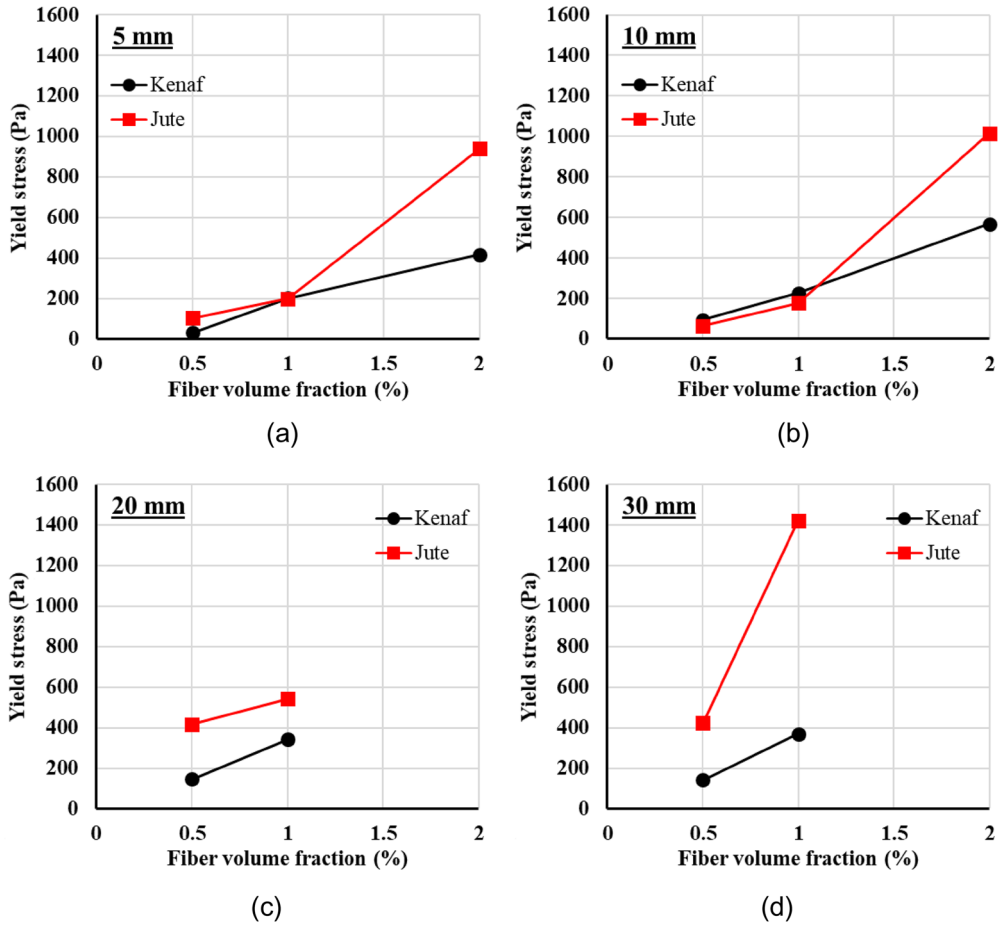

Fig. 10 Yield stress of NFRCCs versus the volume fraction of fibers of different lengths: **a** 5 mm; **b**10 mm; **c** 20 mm; **d** 30 mm

the yield stress is highly dependent on the type of fiber, and the main difference between the fiber types is their surface roughness. For reference, Chin and Yousif (2009) measured the friction coefficients of kenaf and jute fibers, and they obtained values of 0.52–0.65 for the former and 0.75–1.0 for the latter. Thus, it was concluded that the rougher surface of the jute fibers contributed to the higher yield stress of these mixtures (Fig. 10).

3.1.2 Plastic Viscosity

The plastic viscosities of kenaf and jute mixtures were in the ranges 4.5–20 Pa s and 4.5–33 Pa s, respectively (Fig. 11). The overall viscosities of the jute series were higher than those of the kenaf series (Fig. 11), which corresponds to the yield stress results. The rougher surfaces of the jute fibers appear to account for the higher level of plastic viscosity (Chin & Yousif, 2009). However, the effect of fiber length on viscosity was opposite to that observed in the yield stress. Regardless of the type of fiber, the use of longer fibers caused a decrease in the plastic viscosity for a given fiber volume fraction.

At a constant fiber volume fraction, shorter fibers led to greater friction between the matrix and fibers because of their greater total surface area (from the greater number of fibers) compared with longer fibers. For the two plant types, only the mixtures with 30-mm-long fibers showed a notably larger plastic viscosity than those with 20-mm-long fibers; this seemed to be caused by the agglomeration of the 30-mm-long fibers.

For a given fiber length, increasing the fiber volume fraction generally leads to a decrease in the viscosity. This was attributed to an increased lubrication effect with the use of more fibers in the SSD condition (as observed for both cellulose microfibers and superabsorbent polymers (Dang et al., 2017; Gwon & Shin, 2021) as well as the increased number of entrained air bubbles created during the relatively long mixing period of 30 min.

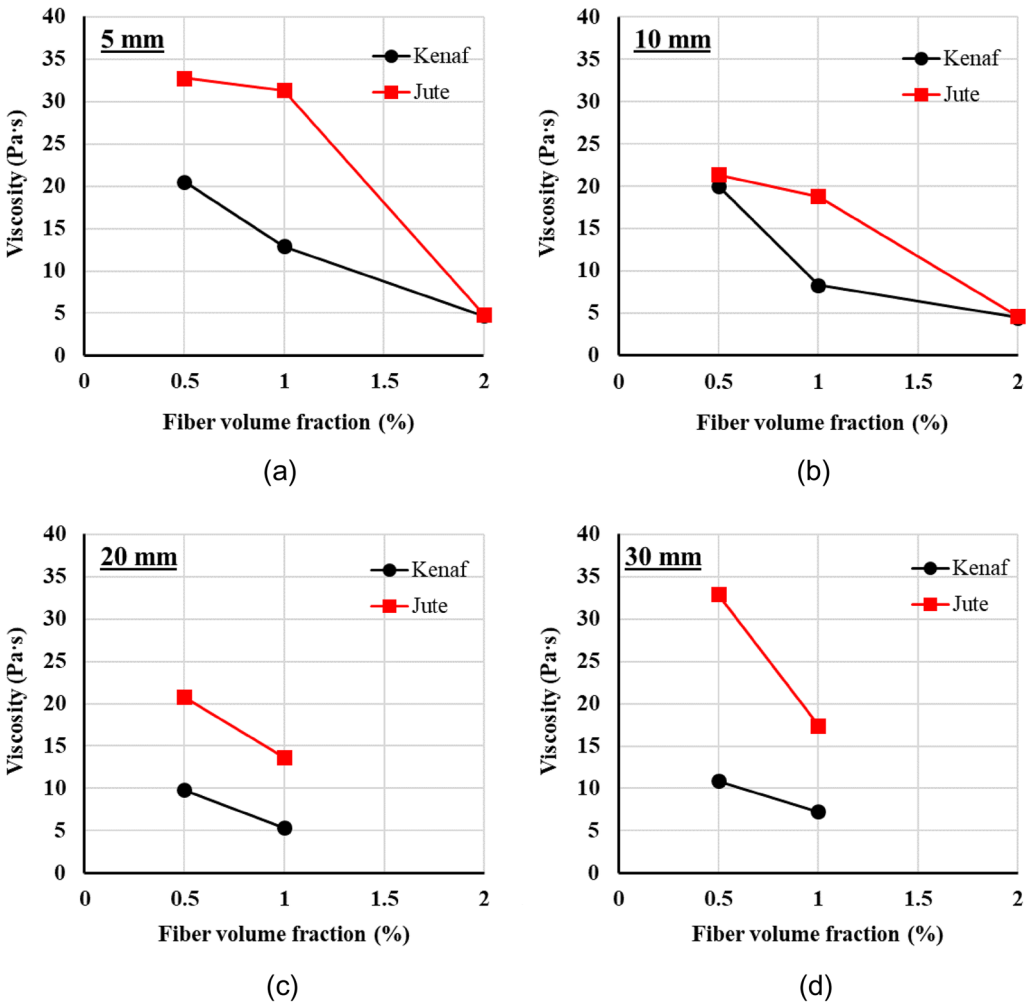

Fig. 11 Plastic viscosity of NFRCCs versus the volume fraction of fibers of different lengths: **a** 5 mm; **b** 10 mm; **c** 20 mm; **d** 30 mm

3.2 Correlation Between Rheological Properties and Air Content

3.2.1 Effect of Natural Fibers on the Air Content

Initially, all mixtures in this study were assumed to contain both intrinsic pores of the fibers and entrained air bubbles created during the relatively long mixing period of 30 min (Mwaikambo & Ansell, 2001; Struble & Jiang, 2004). Overall, for a given fiber length, increasing the volume fraction caused the NFRCCs to have a higher air content with both plant types of fiber (Fig. 12). This was due to the increased porosity from not only the greater fiber volume but also from the increased number of entrained air bubbles. However, at a constant fiber volume fraction, the mixtures with longer fibers (except for the 10-mm-long jute fibers) had lower air content than those with shorter fibers (Fig. 12). This is likely due to the reduction in entrained air bubbles resulting from fewer long fibers despite having the same fiber volume fraction.

3.2.2 Rheological Properties Versus Air Content

Regardless of the type of fiber in all mixtures, the yield stress showed a positive correlation with air content (Fig. 13). Among the two types of fibers, the jute series exhibited a more rapid increase in the yield stress with air content, as evidenced by the steeper trend lines in Fig. 13. This phenomenon was due to the jute fibers having rougher surfaces than the kenaf fibers, which resulted in greater overall rheological properties. For both types of fibers, the effect of the fiber volume fraction on the positive correlation between the yield stress and air content was more pronounced than that of the fiber length. This is because the use of a higher volume of fibers entrains more air bubbles, which are created during the long mixing period of 30 min. For reference, by an air-entraining agent, Struble and Jiang, (2004) found that the yield stress of cement pastes increased when they contained more entrained air bubbles as the bubble bridges formed

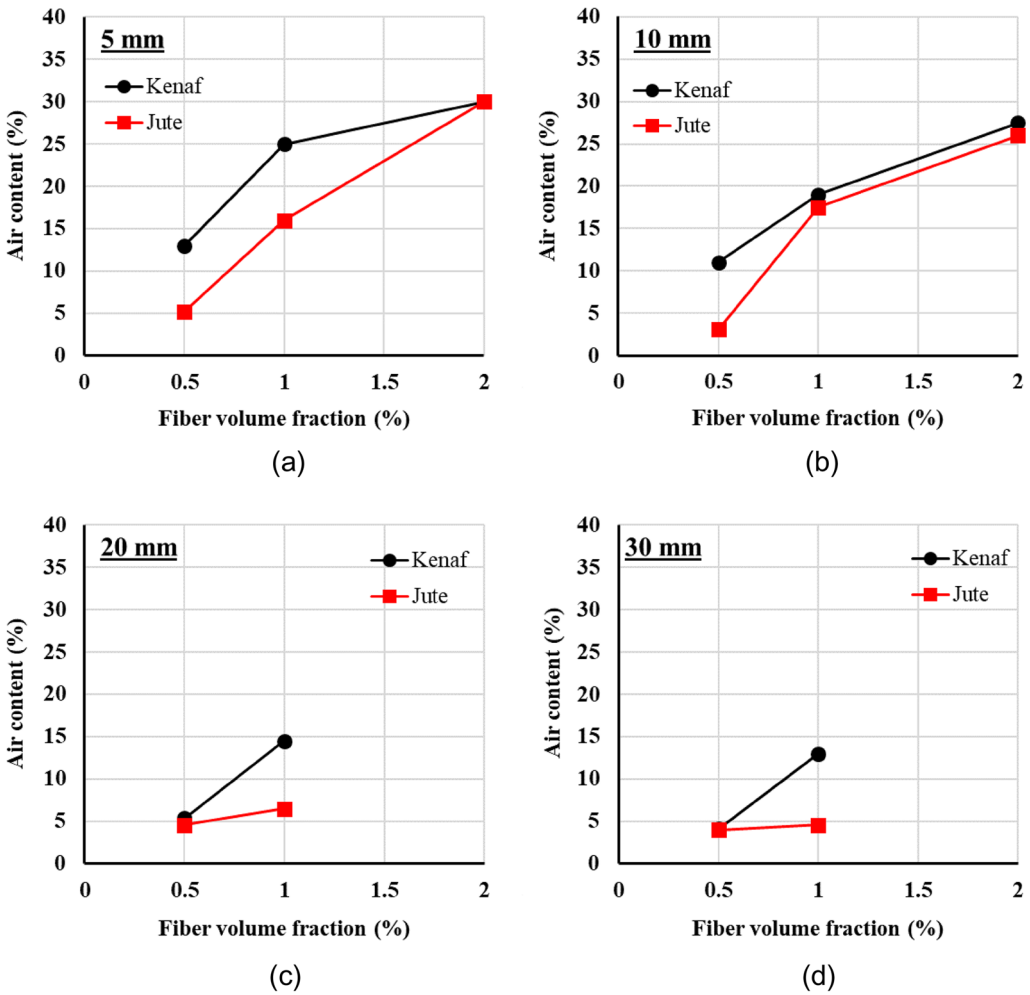

Fig. 12 Air content of NFRCCs versus the volume fraction of fibers of different lengths: **a** 5 mm; **b** 10 mm; **c** 20 mm; **d** 30 mm

between the positively charged cement particles and negatively charged air bubbles prevented the flow of cement pastes. In other words, a greater number of entrained air bubbles from the use of a higher volume fraction of fiber caused more flocculation of particles, inducing an increase in yield stress.

For both types of fibers in all mixtures, the plastic viscosity was negatively correlated to air content (Fig. 14). This correlation was more dependent on the fiber content than on the fiber length, as observed in the positive correlation between the air content and yield stress (Fig. 13). Although the increased number of entrained bubbles owing to the use of a higher volume fraction of fiber led to higher yield stress, they facilitated a lower plastic viscosity once the mixtures started to flow. Therefore, it was concluded that the air bubbles in NFRCCs acted as fluids after yielding (Struble & Jiang, 2004).

3.3 Mechanical Properties

3.3.1 Compressive Strength and Elastic Modulus

Mechanical tests were performed only on the NFRCCs with kenaf fibers to examine the effects of volume fraction and length of the fibers. Overall, as the fiber volume fraction increased from 0.5 to 2.0%, the compressive strength and elastic modulus of the mixtures decreased from 27.5 to 6.0 MPa and from 27.0 to 12.5 GPa, respectively (Fig. 15). Both the intrinsic pores of the fibers and entrained air bubbles created during the mixing period seemed to account for the decrease in these two properties, which was also revealed by the air-content tests. The development trends concerning the fiber content was significantly parallel. This result is also convincing given the general relationship between the strength and porosity of a solid (Neville, 1995; Scrivener et al., 2018). Furthermore, many previous studies have reported that the mechanical properties of NFRCCs deteriorate as the

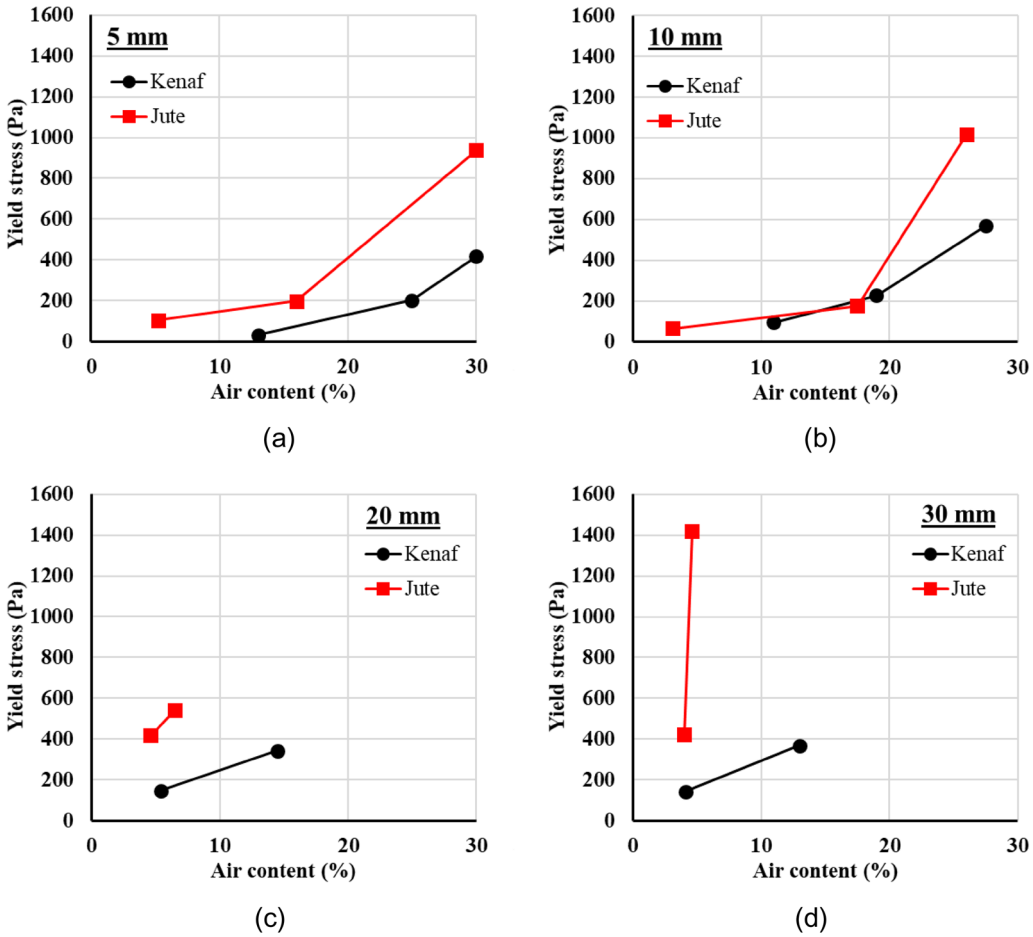

Fig. 13 Correlation between yield stress and air content of NFRCCs for the same fiber length: **a** 5 mm; **b** 10 mm; **c** 20 mm; **d** 30 mm

fiber content increases (Dávila-Pompermayer et al., 2020; Elsaid et al., 2011; Gwon et al., 2021). Jute-fiber series could have exhibited a similar development of compressive strength and elastic modulus to kenaf-fiber series. However, additional tests should be performed in the near future to acquire more accurate results of jute-fiber series. For a given fiber content, the effect of the fiber length on the compressive strength and elastic modulus was not clear, except for mixtures with 0.5% fibers (Fig. 15). It should be noted that all mixtures failed in a ductile manner, as shown by the fiber bridging across the crack faces in Fig. 16. Although Yun et al., (2022) used the same type of kenaf fibers as those used in this study to fabricate NFRCCs, we found no substantial difference in the compressive and flexural strengths at 28 days with respect to the length and content of the fibers, as summarized in Table 2. This was probably due to the use of a water-to-cement ratio of 0.44 and a fiber content of approximately 0.1–0.3 wt. % of cement by Yun et al., (2022); these values were completely different from those used in this study.

3.3.2 Flexural Strength

As with the compressive strength and elastic modulus results, the flexural strengths of the NFRCCs decreased with increasing fiber content at each fiber length (Fig. 17). This was also attributed to the increase in porosity due to the intrinsic pores of the fibers and entrained air bubbles, as discussed above. However, at a given fiber content, the overall effect of the length on the flexural strength was not evident. Jute-fiber series could have exhibited a similar development of flexural strength to kenaf-fiber series, as discussed in the previous section. Excluding the cases of 20 mm fibers, the longer fibers tended to be accompanied by a lower flexural strength at a given fiber content, because a greater number of fibers was available using the shorter ones rather than longer ones, which enabled a superior arrestment of fine cracks under flexure (Pickering et al., 2016).

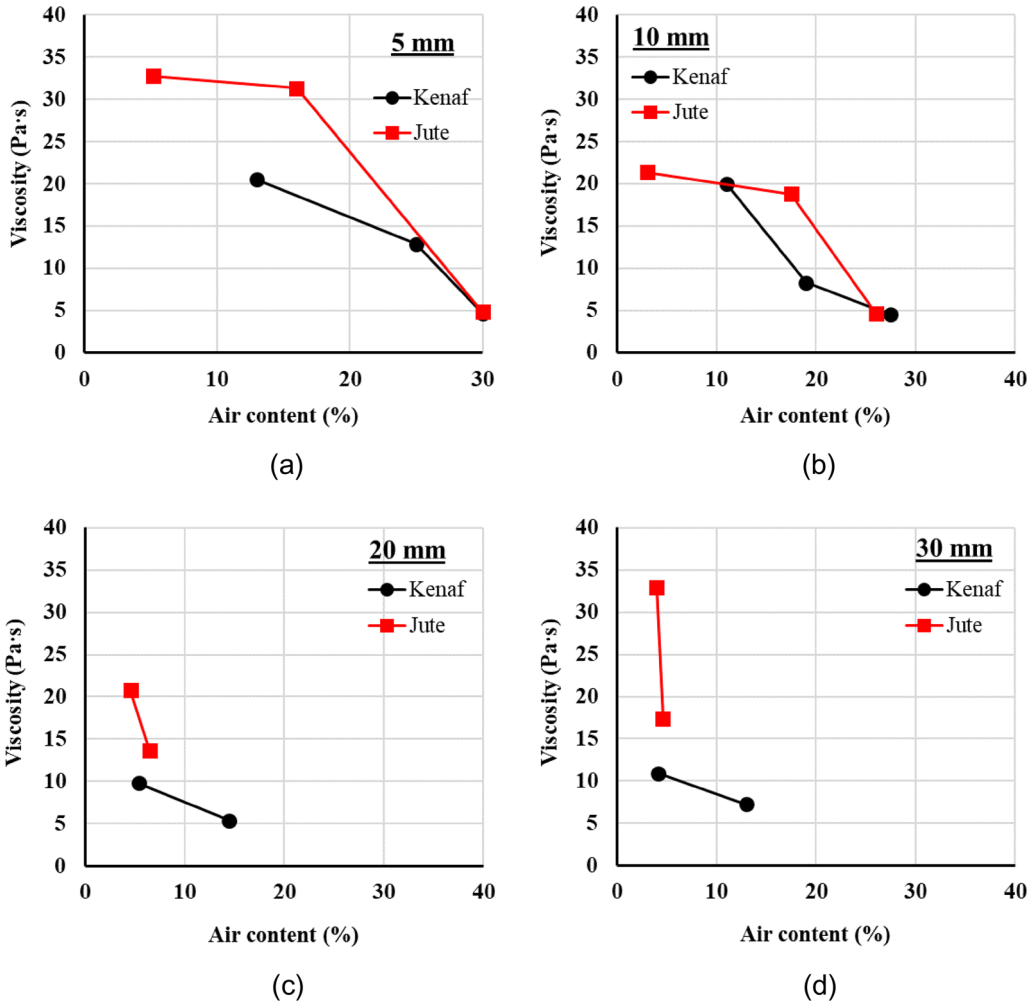

Fig. 14 Correlation between viscosity and air content of NFRCCs for the same fiber length: **a** 5 mm; **b** 10 mm; **c** 20 mm; **d** 30 mm

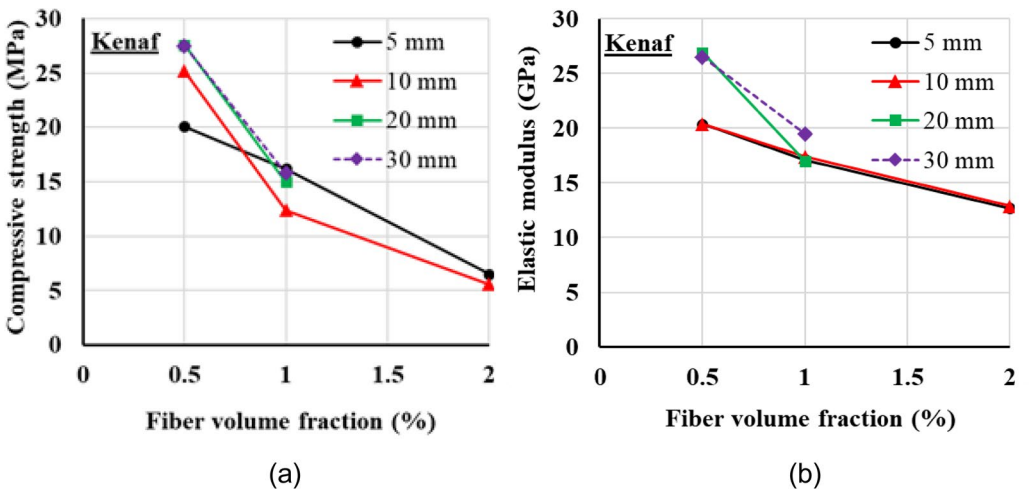

Fig. 15 Effect of kenaf fibers on **a** compressive strength and **b** elastic modulus

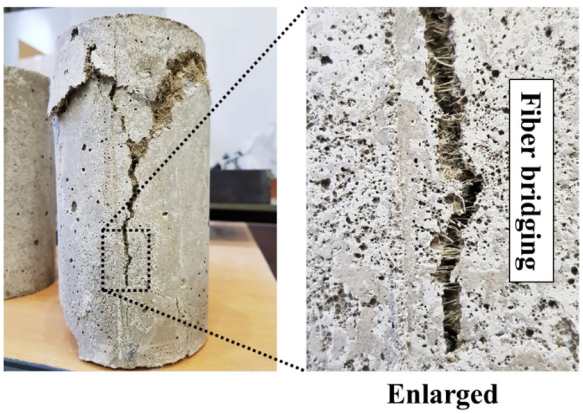

Fig. 16 Failed specimen under compression

3.4 Fiber Dispersion

Using fibers with lengths of 5 mm and 10 mm, the dispersion coefficient of the kenaf fibers increased with increasing fiber volume fraction (Fig. 18), as evidenced by their fluorescence images (Fig. 19a–f), which exhibited a denser distribution with increasing fiber content. Thus, the amount of superplasticizer and condition of the prewetted fibers aided the dispersion of fibers in the varying volume fractions. Despite the increase in the fiber volume fraction, the mixtures containing fibers with lengths of 20 mm and 30 mm did not exhibit a consistent change in their dispersion coefficients. Even with 30-mm-long fibers at a 1% volume fraction, the dispersion coefficient of kenaf fibers decreased abruptly compared to using 0.5% fibers because of the less uniform distribution and local agglomeration of the fibers, as shown in Fig. 19j.

4 Conclusions

This study investigated the rheological and mechanical properties of cement composites with kenaf and jute fibers for use in shotcrete. The main test variables were plant type, length, and volume fraction of the natural fibers. The fresh properties of the NFRCCs were evaluated using rheometer and air-content tests. Their mechanical properties were examined via compression and flexural tests. The degree of fiber dispersion in the NFRCCs was assessed using a fluorescence microscope. The findings and conclusions of this study are summarized as follows:

1. For a given fiber length, the development of yield stress was dependent on the volume fraction, regardless of the fiber type. This was attributed to the increased number of entrained air bubbles around the fibers, which induced a greater attraction between the cement particles and bubbles (i.e., the creation of bubble bridges). Moreover, the effect of the fiber volume fraction on the yield stress was more pronounced than that of fiber length. The rougher

Table 2 Compressive and flexural strengths of NFRCCs from Yun et al., (2022)

Plant type	Fiber		w/c	s/a	SP	AE	Compressive strength (MPa)	Flexural strength (MPa)
	Length (mm)	Wt.% of c (%)			Wt.% of c (%)	Wt.% of SP (%)		
Kenaf	5	0.1	0.44	0.65	0.9	0.1	49.8	7.5
		0.2					52.5	7.7
		0.3					52.1	8.0
	10	0.1					52.9	7.9
		0.2					51.5	7.6
		0.3					52.6	7.7
	20	0.1					51.8	7.5
		0.2					51.8	7.6
		0.3					48.3	7.4
Jute	5	0.1					49.8	8.0
		0.2					51.0	8.3
		0.3					51.8	8.0
	10	0.1					50.0	8.0
		0.2					50.8	8.5
		0.3					49.2	7.4
	20	0.1					51.4	7.2
		0.2					49.8	7.3
		0.3					50.8	7.2

AE air-entraining agent

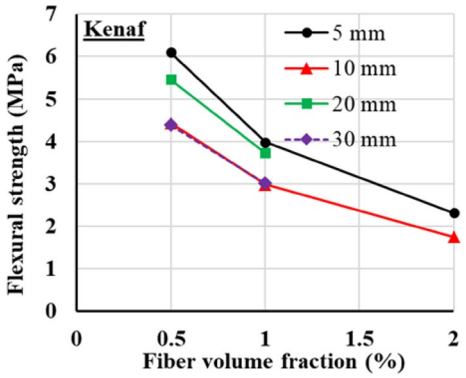

Fig. 17 Effect of kenaf fibers on flexural strength

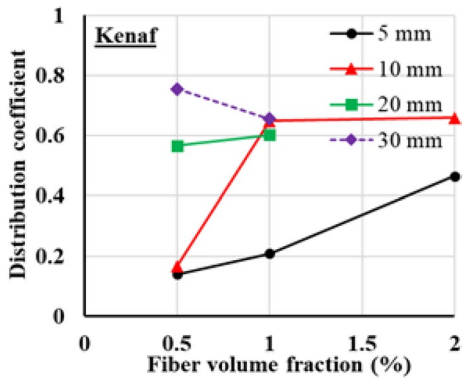

Fig. 18 Distribution coefficient versus volume fraction of kenaf fibers of different lengths

surface of the jute fibers contributed to a higher level of yield stress compared with the relatively smoother kenaf fibers.

2. The level of plastic viscosity was higher when using jute fibers than kenaf fibers. This suggests that the type of fiber affects the rheological properties. Contrary to the development of yield stress, the plastic viscosity of NFRCCs generally decreased with a higher fiber content. This was attributed to the fluid action of the entrained air bubbles as well as the lubrication effect of the fibers in the SSD condition after flow initiation. Thus, it was concluded that the entrained air bubbles in the NFRCCs acted as bubble bridges and fluids before and after the flow initiation, respectively.
3. From the rheological results, the use of 10-mm-long jute fibers at 2% by volume was assumed to allow optimal rheological properties for shotcrete. However, the use of 30-mm-long jute fibers at 1% by volume showed the worst rheological values because of fiber agglomeration.

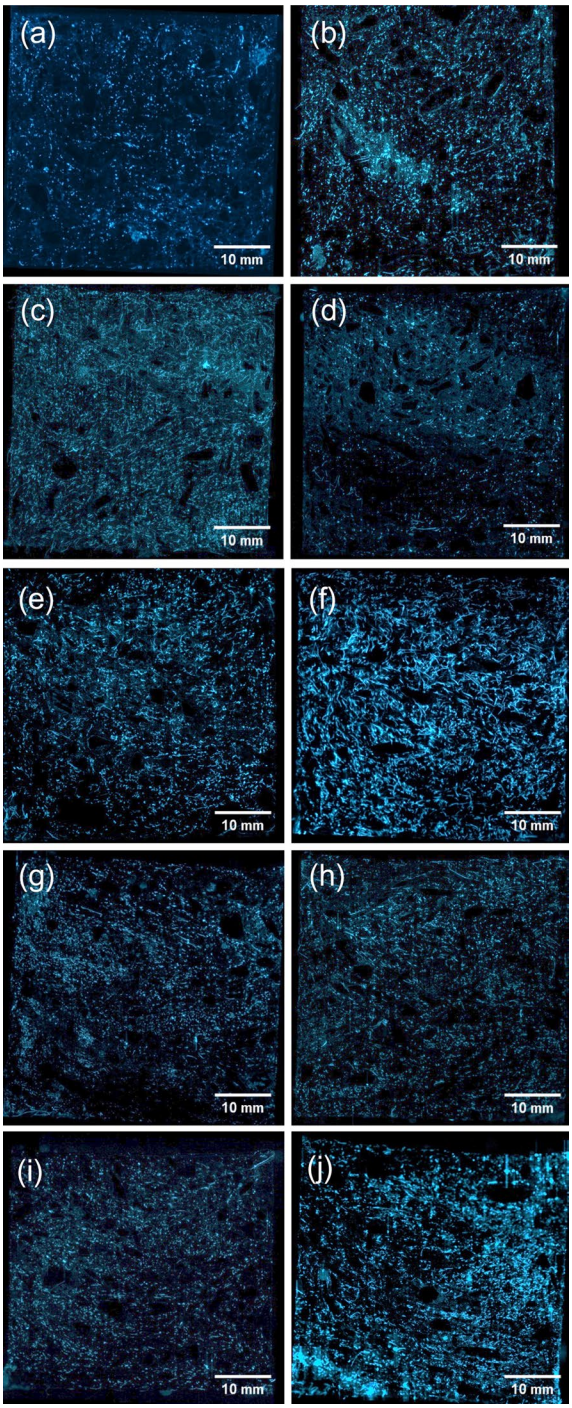

Fig. 19 Fluorescence images of natural fiber-reinforced concrete with kenaf fibers: **a** 5 mm, 0.5%; **b** 5 mm, 1.0%; **c** 5 mm, 2.0%; **d** 10 mm, 0.5%; **e** 10 mm, 1.0%; **f** 10 mm, 2.0%; **g** 20 mm, 0.5%; **h** 20 mm, 1.0%; **i** 30 mm, 0.5%; **j** 30 mm, 1.0%

4. The porosities of all the mixtures was due to the intrinsic pores of the natural fibers and entrained air bubbles. For a given fiber length, the yield stress and plastic viscosity exhibited positive and negative correlations with the air content of all mixtures, respectively. Both rheological properties were observed to depend primarily on the fiber volume fraction.
5. Although the dispersion coefficient increased with increasing fiber volume fraction, all the mechanical properties of NFRCCs (compressive strengths of 27.5 to 6 MPa, elastic moduli of 27 to 12.5 GPa, flexural strengths of 6.2 to 1.8 MPa) deteriorated as the fiber content increased. This observation was convincing, given the general relationship between the strength and porosity of a solid. However, for a given fiber volume fraction, the effect of fiber length on the mechanical properties was not clear.

Declarations

Ethics approval and consent to participate
The authors state that the research was conducted according to ethical standards.

Consent for publication
The authors consent for publication.

Competing interests
The authors declare that they have no competing interests in this work.

Author details
[1]School of Civil and Environmental Engineering, Hankyong National University, 327 Jungang-ro, Anseong, Gyeonggi-do 17579, Republic of Korea. [2]Department of Civil and Environmental Engineering, Korea Advanced Institute of Science and Technology, 291 Daehak-ro, Yuseong-gu, Daejeon 34141, Republic of Korea. [3]Department of Urban and Environmental Engineering, Ulsan National Institute of Science and Technology (UNIST), 50 UNIST-Gil, Ulsan 44919, Republic of Korea. [4] Construction Engineering Research Institute, Hankyong National University, 327 Jungang-ro, Anseong, Gyeonggi-do 17579, Republic of Korea.

Received: 30 April 2022 Accepted: 3 October 2022
Published online: 24 January 2023

Abbreviations
a: Aggregate; c: Cement; h: Vane height; N: Number of sections in a plane; R_1: Vane radius; R_2: Outer container radius; s: Sand; T: Torque applied by vane; w: Water; w*: Effective water; $\overline{X}$: Total number of fibers in the plane; X_i: Number of fibers in the ith square-shaped section; α_f: Distribution coefficient; $\dot{\gamma}$: Shear strain rate; μ: Plastic viscosity; τ: Shear stress; τ_0: Yield stress; Ω: Vane rotation speed; $\Phi(X)$: Coefficient of variation.

Acknowledgements
Not applicable

Author contributions
SG: conceptualization, methodology, investigation, validation, formal analysis, investigation, data curation, writing—original draft preparation, writing—review and editing, visualization; SHH: methodology, investigation, validation, formal analysis, data curation; TDV: formal analysis, data curation; CK: formal analysis, data curation; MS: writing—review and editing, resources, supervision, project administration, and funding acquisition. All authors have read and agreed to the published version of the manuscript. All authors read and approved the final manuscript.

Authors' information
Seongwoo Gwon: Assistant Professor at Hankyong National University, 327 Jungang-ro, Anseong-si, Gyeonggi-do 17579, Republic of Korea. Seong Ho Han: Postdoctoral Researcher at Korea Advanced Institute of Science and Technology, 291 Daehak-ro, Yuseong-gu, Daejeon 34141, Republic of Korea. Thanh Duc Vu: Master's student at Ulsan National Institute of Science and Technology (UNIST), 50 UNIST-gil, Ulsan 44919, Republic of Korea. Chanyoung Kim: PhD Candidate at Ulsan National Institute of Science and Technology (UNIST), 50 UNIST-gil, Ulsan 44919, Republic of Korea. Myoungsu Shin: Professor at Ulsan National Institute of Science and Technology (UNIST), 50 UNIST-gil, Ulsan 44919, Republic of Korea.

Funding
This research was supported by grants from the Mid-Career Research Program [Grant No. NRF-2022R1A2C2006867] and the Basic Research Lab Program [Grant No. NRF-2021R1A4A1030867] through the National Research Foundation of Korea, which is funded by the Ministry of Science and ICT.

Availability of data and materials
The data and materials are included in the manuscript.

References
ACI (American Concrete Institute). (2016). *Guide to Shotcrete*. American Concrete Institute, Farmington Hills, MI, USA.
Ahn, E., Shin, M., (2018). Effects of moisture contents on the diffusion of ultrasound in concrete. Proceedings of 12th fib PhD Symposium in Civil Engineering, Prague, Czech Republic. pp. 947–952
Amiri, A., Triplett, Z., Moreira, A., Brezinka, N., Alcock, M., & Ulven, C. A. (2017). Standard density measurement method development for flax fiber. *Industrial Crops and Products, 96*, 196–202.
ASTM. (2019). C1609/C1609M-19a: Standard test method for flexural performance of fiber-reinforced concrete (using beam with third-point loading). *ASTM International, West Conshohocken, PA,*. https://doi.org/10.1520/c1609_c1609m-19a
ASTM. (2020a). C150/C150M-20: Standard specification for Portland cement. *ASTM International, West Conshohocken, PA,*. https://doi.org/10.1520/c0150_c0150m-20
ASTM. (2020b). C185-20: Standard test method for air content of hydraulic cement mortar. *ASTM International, West Conshohocken, PA,*. https://doi.org/10.1520/c0185-20
ASTM. (2020c). C39/C39M-20: Standard test method for compressive strength of cylindrical concrete specimens. *ASTM International, West Conshohocken, PA*. https://doi.org/10.1520/c0039_c0039m-20
Awwad, E., Mabsout, M., Hamad, B., Farran, M. T., & Khatib, H. (2012). Studies on fiber-reinforced concrete using industrial hemp fibers. *Construction and Building Materials, 35*, 710–717.
Banthia, N. (2019). Advances in sprayed concrete (shotcrete). In *Developments in the Formulation and Reinforcement of Concrete* (pp. 289–306). Woodhead Publishing
Beaupré, D. (1994). *Rheology of High-performance Shotcrete*. PhD thesis, The University of British Columbia
Bingham, E. C. (1916). An investigation of the laws of plastic flow. *Bulletin of the Bureau of Standards, 13*(2), 309–353. https://doi.org/10.6028/bulletin.304
Chin, C. W., & Yousif, B. F. (2009). Potential of kenaf fibers as reinforcement for tribological applications. *Wear, 267*(9–10), 1550–1557.
Choi, H., & Choi, Y. C. (2021). Setting characteristics of natural cellulose fiber reinforced cement composite. *Construction and Building Materials, 271*, 121910.
Dang, J., Zhao, J., & Du, Z. (2017). Effect of superabsorbent polymer on the properties of concrete. *Polymers, 9*(12), 672.
Dávila-Pompermayer, R., Lopez-Yepez, L. G., Valdez-Tamez, P., Juárez, C. A., & Durán-Herrera, A. (2020). Lechugilla natural fiber as internal curing agent

in self compacting concrete (SCC): Mechanical properties, shrinkage, and durability. *Cement and Concrete Composites, 112*, 103686.
de Andrade, S. F., Mobasher, B., & Toledo Filho, R. D. (2010). Fatigue behavior of sisal fiber reinforced cement composites. *Materials Science and Engineering: A, 527*(21–22), 5507–5513.
Elsaid, A., Dawood, M., Seracin, R., & Bobko, C. (2011). Mechanical properties of kenaf fiber reinforced concrete. *Construction and Building Materials, 25*(4), 1991–2001.
Fan, M., Ndikontar, M. K., Zhou, X., & Ngamveng, J. N. (2012). Cement-bonded composites made from tropical woods: Compatibility of wood and cement. *Construction and Building Materials, 36*, 135–140.
Gwon, S., Choi, Y. C., & Shin, M. (2021). Effect of plant cellulose microfibers on the hydration of cement composites. *Construction and Building Materials, 267*, 121734.
Gwon, S., Choi, Y. C., & Shin, M. (2022). Internal curing of cement composites using kenaf cellulose microfibers. *Journal of Building Engineering, 47*, 103867. https://doi.org/10.1016/j.jobe.2021.103867
Gwon, S., & Shin, M. (2021). Rheological properties of cement pastes with cellulose microfibers. *Journal of Materials Research and Technology, 10*, 808–818.
Jongvisuttisun, P., Leisen, J., & Kurtis, K. E. (2018). Key mechanisms controlling internal curing performance of natural fibers. *Cement and Concrete Research, 107*, 206–220.
Kanda, T., & Li, V. C. (1998). Interface property and apparent strength of the high-strength hydrophilic fiber in a cement matrix. *Journal of Materials in Civil Engineering, 10*(1), 5–13.
Koehler, E. P., Fowler, D. W. (2004). *Development of a Portable Rheometer for Fresh Portland Cement Concrete*, ICAR Report 105-3F
Kostrzanowska-Siedlarz, A., & Gołaszewski, J. (2015). Rheological properties and the air content in fresh concrete for self-compacting high-performance concrete. *Construction and Building Materials, 94*, 555–564.
Li, V. C., & Obla, K. H. (1994). Effect of fiber length variation on tensile properties of carbon-fiber cement composites. *Composites Part b: Engineering, 4*(9), 947–964.
Li, X., Tabil, L. G., & Panigrahi, S. (2007). Chemical treatments of natural fiber for use in natural fiber-reinforced composites: A review. *Journal of Polymers and the Environment, 15*(1), 25–33.
Li, Z., Wang, L., & Wang, X. (2004). Compressive and flexural properties of hemp fiber reinforced concrete. *Fibers and Polymers, 5*(3), 187–197.
Li, Z., Wang, L., & Wang, X. (2006). Flexural characteristics of coir fiber reinforced cementitious composites. *Fibers and Polymers, 7*(3), 286–294.
MacVicar, R., Matuana, L. M., & Balatinecz, J. J. (1999). Aging mechanisms in cellulose fiber reinforced cement composites. *Cement and Concrete Composites, 21*(3), 189–196.
Market Research Future. (2009). Cellulose fiber market: information by fiber type. Application and region—forecast till 2025. Retrieved November 10, 2020, from https://www.marketresearchfuture.com/reports/cellulose-fiber-market-2903/
Mezencevova, A., Garas, V., Nanko, H., & Kurtis, K. E. (2012). Influence of thermo-mechanical pulp fiber compositions on internal curing of cementitious materials. *Journal of Materials in Civil Engineering, 24*(8), 970–975.
Morgan, D.R., Zhang, L., & Pildysh, M. (2017). New hemp-based fiber enhances wet-mix shotcrete performance. *Shotcrete* Spring
Mwaikambo, L. Y., & Ansell, M. P. (2001). The determination of porosity and cellulose content of plant fibers by density methods. *Journal of Materials Science Letters, 20*(23), 2095–2096.
Neville, A. M. (1995). *Properties of Concrete* (4th ed.). Longman.
Onuaguluchi, O., & Banthia, N. (2016). Plant-based natural fibre reinforced cement composites: A review. *Cement and Concrete Composites, 68*, 96–108.
Pacheco-Torgal, F., & Jalali, S. (2011). Cementitious building materials reinforced with vegetable fibres: A review. *Construction and Building Materials, 25*(2), 575–581.
Pickering, K. L., Efendy, M. A., & Le, T. M. (2016). A review of recent developments in natural fiber composites and their mechanical performance. *Composites Part a: Applied Science and Manufacturing, 83*, 98–112.
Ramakrishna, G., & Sundararajan, T. (2005). Impact strength of a few natural fiber reinforced cement mortar slabs: A comparative study. *Cement and Concrete Composites, 27*(5), 547–553.
Roma, L. C., Martello, L. S., & Savastano, H. (2008). Evaluation of the mechanical, physical, and thermal performance of cement-based tiles reinforced with vegetable fibers. *Construction and Building Materials, 22*(4), 668–674.
Saheb, D. N., & Jog, J. P. (1999). Natural fiber polymer composites: A review. *Advances in Polymer Technology, 18*(4), 351–363.
Sawsen, C., Fouzia, K., Mohamed, B., & Moussa, G. (2014). Optimizing the formulation of flax fiber-reinforced cement composites. *Construction and Building Materials, 54*, 659–664.
Sawsen, C., Fouzia, K., Mohamed, B., & Moussa, G. (2015). Effect of flax fibers treatments on the rheological and the mechanical behavior of a cement composite. *Construction and Building Materials, 79*, 229–235.
Scrivener, K., Snellings, R., & Lothenbach, B. (2018). *A Practical Guide to Microstructural Analysis of Cementitious Materials*. CRC Press.
Singh, M., Saini, B., & Chalak, H. D. (2019). Performance and composition analysis of engineered cementitious composite (ECC): A review. *Journal of Building Engineering, 26*, 100851.
Struble, L. J., & Jiang, Q. (2004). Effects of air entrainment on rheology. *ACI Materials Journal, 101*(6), 448–456.
Torigoe, S. I., Horikoshi, T., Ogawa, A., Saito, T., & Hamada, T. (2003). Study on evaluation method for PVA fiber distribution in an engineered cementitious composite. *Journal of Advanced Concrete Technology, 1*(3), 265–268.
Vaickelionis, G., & Vaickelioniene, R. (2006). Cement hydration in the presence of wood extractives and pozzolan mineral additives. *Ceramics Silikaty, 50*(2), 115–122.
Valadez-Gonzalez, A., Cervantes-Uc, J. M., Olayo, R. J. I. P., & Herrera-Franco, P. J. (1999). Effect of fiber surface treatment on the fiber–matrix bond strength of natural fiber-reinforced composites. *Composites Part b: Engineering, 30*(3), 309–320.
Wei, J., & Meyer, C. (2014). Sisal fiber-reinforced cement composite with Portland cement substitution by a combination of metakaolin and nanoclay. *Journal of Materials Science, 49*(21), 7604–7619.
Yun, K. K., Hossain, M. S., Han, S., & Seunghak, C. (2022). Rheological, mechanical properties, and statistical significance analysis of shotcrete with various natural fibers and mixing ratios. *Case Studies in Construction Materials, 16*, e00833.
Zhu, W. H., Tobias, B. C., Coutts, R. S. P., & Langfors, G. (1994). Air-cured banana-fibre-reinforced cement composites. *Cement and Concrete Composites, 16*(1), 3–8.

Publisher's Note